COOLING ELECTRONS IN FAR FIELD OF PLUME PLASMA

Boris Vayner
Ohio Aerospace Institute, Cleveland, Ohio 44142, USA, E-mail: Boris.V.Vayner@nasa.gov

ABSTRACT

New NASA project includes powerful plasma thruster (300 kW) and high-voltage solar array providing approximately 350 kW of electric power at distances about 1 AU from the Sun. Plasma thruster generates comparatively dense plasma that interacts with solar array, and these interactions may cause some detrimental consequences such as parasitic current collection, surface sputtering, additional torque, etc. Besides these factors the performance of a high-voltage (over 300 V) solar array in natural and generated environments was never studied before. In order to perform respective tests in vacuum vessels one needs to know the parameters of plume plasma in very far field. There are two complimentary approaches to the search for solution of this problem: 1) performing extensive computer simulations; 2) measuring plasma parameters in ground chambers. Plume plasma parameters in chamber and space are different, and the quantitative characteristics of these differences were analyzed in this paper.

Electric propulsion systems have been used for space exploration for a long time. Recently, the deployment of Solar Electric Propulsion come up to consideration for a manned mission to astronomical bodies. Taking into account the highest solar cell efficiencies achieved to date one can estimate the area of prospective array as of 800-900 m^2. Adequate testing of solar array coupons in plume plasma demands understanding the differences between spatial distributions of plasma parameters in space and in vacuum chamber. Such factors as backpressure of neutral gas and vessel walls influence on plasma density, plasma potential, and electron temperature. The quantitative characteristics of these differences for any thruster depend on chamber dimensions and pumping speed. Voluminous arrays of data were obtained experimentally for various types of plasma thrusters operated in diverse chambers, and common conclusions were accepted: electron temperature decreased with distance from thruster orifice and increased with the background pressure decreasing. Plume plasma electron temperature is very important parameter for evaluating the interactions between spacecraft elements and thruster plume. All measurements performed in vacuum chambers indicated rather low electron temperatures (0.5-2 eV) in far field while computer simulations and measurements in space (one only) pointed to significantly higher temperatures (3-6 eV). The physical mechanisms of electron cooling in far field were not understood because of seemly collisionless electron gas in a vessel. It is shown in current paper that electron cooling in plasma chamber is caused by creation of potential barrier near walls, and this barrier originates from self-organization of electrically neutral plasma.

1. INTRODUCTION

Electric propulsion systems have been used for space exploration for a long time. Recently, the deployment of Solar Electric Propulsion come up to consideration for a manned mission to astronomical bodies [1]. This project includes powerful plasma thruster (300 kW) and high-voltage solar array providing approximately 350 kW of electric power at distances about 1 AU from the Sun. Taking into account the highest solar cell efficiencies achieved to date one can estimate the area of prospective array as of 800-900 m^2. Plasma thruster generates comparatively dense plasma that interacts with solar array, and these interactions may cause some detrimental consequences such as parasitic current collection, surface sputtering, additional torque, etc. Besides these factors the performance of a high-voltage (over 300 V) solar array in natural and generated environments was never studied before. In order to perform respective tests in vacuum vessels one needs to know the parameters of plume plasma in very far field. There are two complimentary approaches to the search for solution of this problem: 1) performing extensive computer simulations; 2) measuring plasma parameters in ground chambers. These two approaches are mutually intertwined, but the results are frequently contradictive. Generally speaking, plume plasma parameters in chamber and space are different: backpressure of neutral gas and a vessel walls influence on plasma density, plasma potential, and electron temperature. The quantitative characteristics of these differences for any thruster depend on chamber dimensions and pumping speed.

The comprehensive study of all these factors was performed in [2]. Background pressure (Xenon) varied from 3.5 μTorr to 73 μTorr. The electron temperature variations at the distance of 1 m from thruster exit plane (at the angle of 50 deg from axis) were determined within the range of 1-2 eV for floating thruster and 0.9-1.3 eV for thruster grounded. The electron temperature increased with pressure decreasing, and measurements error was estimated at

20%. In order to establish adequate test conditions the influence of a test arrangement on plume plasma parameters was analyzed and some criteria for appropriate ground test conditions were presented.

2. GROUND EXPERIMENTS

The effect of backpressure was studied for P5 Hall thruster in a quite large chamber with a diameter of 6 m and length of 9 m [3]. Two sets of measurements were performed at xenon background pressures of 3.6 μTorr and 11 μTorr. Probes were positioned at the distance of 1 m from exit plane, which was equal to seven thruster diameters approximately (D_0=148 mm). Certainly, ion current density was decreased about two times with increased pressure, and electron number density demonstrated dependence on pressure with factors of 2-4. Electron temperature varied within the range of T_e=1.2-1.6 eV, and no correlations were established between electron temperature and neutral gas pressure.

Plasma properties of Electron Cyclotron Resonance (ECR) thruster in the near field (2 cm from exit plane) were investigated in Ref.4. Measurements were performed by probes moving in radial direction (-50 cm<y<50 cm), and there was revealed practical independence of electron temperature on input power (P=0.9-1.6 kW). However, electron temperature was decreasing with increasing flow rate: T_e=2.5-3 eV at $\dot{m} = 20\,sccm$, and T_e=1.3-2.3 eV at $\dot{m} = 36\,sccm.$ These results were obtained in fairly large chamber (D=2.2 m, L=7.9 m), and they confirmed that low electron temperatures were caused by processes inside thruster but not the influence of background gas pressure.

Plasma plume properties of the cluster of four BHT-200 Hall thrusters were measured at the distances comparable with assembly dimensions [5]. Electron number density and electron temperature dropped from n_e=10^{12} cm^{-3} and T_e=3 eV to n_e=3*10^{10} cm^{-3} and T_e=1 eV when the distance from exit plane was increased from z=5 cm to z=25 cm. This experiment was conducted in a chamber with diameter D=1.8 m and length L=3 m under background pressure of 23 μTorr. Because of comparatively high neutral gas pressure the influence of neutral xenon on plasma parameters needs a special investigation.

Somewhat higher electron temperatures were recorded in far field for 1.5 kW Hall thrusters (PPS-100ML and PPI) [6]. This experiment was conducted in a chamber with diameter D=2.2 m and length L=4m under background pressure of 7.5 μTorr. Electron temperature dropped from T_e=4.6 eV to T_e=3.4 eV when axial distance increased from z=30 cm to z=50 cm (from $3D_0$ to $5D_0$). Electron number densities decreased from n_e=3.5*10^{10} cm^{-3} to n_e=1.2*10^{10} cm^{-3} within the same range of the distances. The attempt to fit measurements with respective polytropic equation resulted in exponent of γ=1.38-2.18. The value of γ>1.67 meant additional cooling mechanism that was not elaborated in this work.

Plasma parameters were measured in the near field plume of NASA-300M (20 kW) Hall thruster [7]. The tests were performed in large chamber (D=4.6 m and L=18.3 m) equipped with twenty diffusion pumps. Facility base pressure of 0.4 μTorr was kept steady during the test. Neutral gas pressure near the thruster exit plane did not exceed 25 μTorr. Electron temperatures depended on thruster operational parameters but at the distances of $2D_0$ in both axial and radial directions the temperatures were in the range of 1-3 eV.

Electrostatic probes were used to measure plasma parameters inside the discharge channel of SPT-50 Hall thruster [8]. Electron temperatures reached 8-12 eV at the channel exit, and the temperature increased with rising discharge voltage. It was shown that xenon flow rate influenced electron distribution function rather weakly. These tests were conducted in a small chamber (D=0.8 m and L=1.8 m) with a base pressure of 37-60 μTorr. Far field plasma parameters were measured in a larger chamber (D=1.8 m and L=2 m) [9]. The spatial distributions of electron number densities and electron temperatures were obtained in vertical plane distanced at 120 cm ($24D_0$) from thruster (Fig.1).

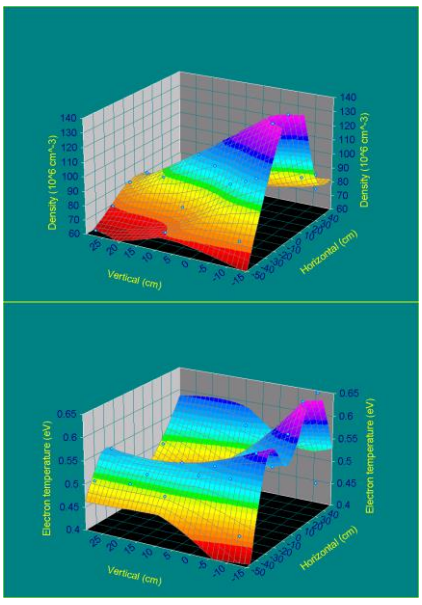

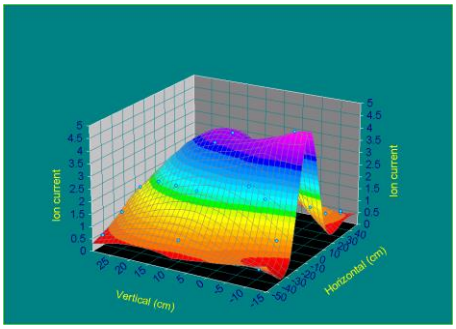

c)

Figure 1. Spatial distributions of plume plasma parameters in vertical plane distanced at 120 cm from SPT-50: top- electron number density; middle- electron temperature; bottom-ion beam current density.

After many attempts to get the highest electron temperature one final set of SPT-50 operational parameters was chosen: power of P=200 W, and flow rate of 4.5 sccm (0.44 mg/s). Working neutral gas pressure was 6 μTorr (corrected for xenon), and temperature changed from 17-21 °C to 25 °C for 7 hour operational time span. It is seen in Fig.1 that electron temperature varied in relatively narrow limits of 0.4-0.65 eV in spite of much more significant variations of number density. There was not possible to determine any correlations between temperature and density for all data obtained in the test (Fig.2).

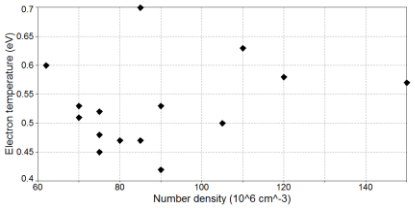

Figure 2. Electron temperature vs. number density for all data obtained.

Thus, it is necessary to explain the decrease in electron temperature from 8-12 eV to 0.4-0.6 eV over one meter distance. In other words, the physical mechanism of electron gas cooling should be identified and analyzed quantitatively.

3. MODEL AND SIMULATIONS

Plume plasma consists of three main components: electrons, ions, and neutral atoms. In order to obtain a detailed picture of spatial distribution of plasma parameters the set of equations for each component and electric field is supposed to be solved [10-13]. Electron number density and electron temperature are two parameters that determine current collection by solar array positioned in a very far field. For example, in case of planned NASA mission [1] both radial and axial distances of over four meters are considered: $r,z>>D_0$.

Due to low ratio of bulk speed of electrons to the thermal speed the dynamic equation for electrons can be written as really static:

$$en_e \frac{\partial \Phi}{\partial \vec{r}} = \frac{\partial p_e}{\partial \vec{r}} \qquad (1)$$

This Eq.(1) can be easily solved for isothermal electrons (T_e= Const):

$$n_e(\vec{r}) = n_{e0} \cdot \exp\left(\frac{e\Phi(\vec{r})}{kT_e}\right) \qquad (2)$$

However, all measurements performed to date demonstrated the dependence of electron temperature on spatial coordinates: sharp drop from 20-30 eV to 4-8 eV near exit plane and slow decrease to 1-3 eV over a scale of 1-2 m. This long scale temperature gradient might be caused by interactions of electrons with background gas in plasma chamber [13], and/or by high thermal conductivity of electron plasma.

For stationary plasma ($\frac{\partial}{\partial t} = 0$) the equation for electron temperature can be written in the following form [14]:

$$\vec{V}_e\left(\frac{3}{2} n_e \frac{\partial T_e}{\partial \vec{r}} - T_e \frac{\partial n_e}{\partial \vec{r}}\right) = -\frac{\partial \vec{q}_e}{\partial \vec{r}} + \sum_{i,j} (\pi_e)_{ij} \frac{\partial \vec{V}_{ei}}{\partial r_j} + Q_e \qquad (3)$$

Where

$$Q_e = -\sum_{\beta} \int \frac{m_e c_e^2}{2} S_{e\beta} \cdot d\vec{v}_e \qquad p_e = k n_e T_e;$$

$$(\pi_e)_{ij} = m_e n_e \left(\frac{\langle c_e^2 \rangle}{3} \delta_{ij} - \langle c_{ei} c_{ej} \rangle\right)$$

Thermal flux is proportional to the temperature gradient:

$$q_{ei} = \sum_j \chi_{eij} \frac{\partial T_e}{\partial r_j} \qquad (4)$$

The thermal conductivity tensor χ_{eij} has different diagonal components and non-vanishing other components if magnetic field is strong enough to be taken into account. Magnetic field strength was measured at the plane distanced at 1.2 m from thruster exit (Fig.3). It is seen in Fig.3 that magnetic field strength is equal to Earth's one, and magnetic field effects will be disregarded in further analysis.

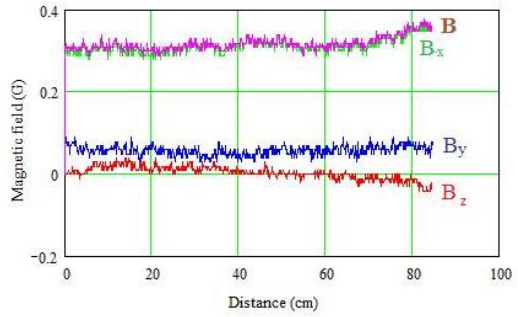

Figure 3. Magnetic field strength vs. horizontal coordinate.

Contribution to the energy balance due to collisions with other species (ions and neutrals) Q_e is determined by the corresponding cross-sections and will be discussed below. Eq.3 was simplified by disregarding for energy transfer from electrons to ions (neutrals) by elastic collisions and by omitting the term with ohmic heating. Full equation for electron component thermal balance was solved in Ref. 11. It was shown that in far field $r,z>8D_0$ the electron temperature dropped to constant value of 2 eV with electron number density in the range of n_e=(1-3)*10^{10} cm^{-3}. It should be stressed that Eq.3 is valid in the area where electron free path is much shorter than the scale of density and temperature variations. Electron free path depends on temperature and number density

$$l_{ee} = \frac{2\cdot 10^{13}}{n_e \ln\Lambda} T_e^2 \; cm \qquad (5)$$

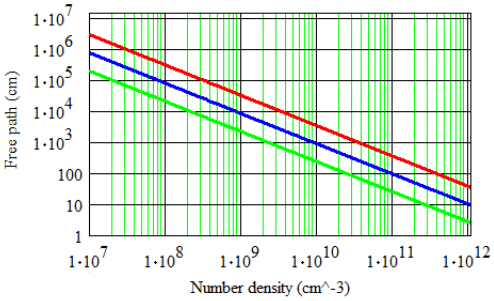

Figure 4. Electron free path vs. number density for T_e=4, 2, and 1 eV.

For plasma density of 10^{10} cm^{-3} and temperature of 2 eV ($r,z>8D_0$) the electron free path is approximately equal to 10 m that is much longer than dimensions of simulation domain. Thus, strictly speaking simulations [11] are valid for the near field area but they reflect (at least qualitatively) the general tendency of decreasing electron temperature from 20-30 eV at exit plane to 2 eV at the distances of a few thruster diameters.

The contribution of thermal conductivity term to the balance equation (3) is characterized by one dimensionless parameter *Pe* -Peclet number:

$$Pe = \frac{V_e n_e k L_t}{\chi_e} \qquad (6)$$

Where thermal conductivity is

$$\chi_e = 4\cdot 10^4 T_e^{5/2} \left(\ln\Lambda\right)^{-1} erg/s\cdot cm\cdot K$$

L_t is a characteristic length of temperature/density gradient, and V_e is electron bulk speed. Substituting measured magnitudes of

$$n_e = 10^{10}\, cm^{-3}, \quad V_e = 10\, km/s, \quad and\; L_t = 1 \quad m$$

one can obtain the estimate for Peclet number:

$$Pe = 10^{-3} T_e^{-5/2} << 1 \qquad (7)$$

It might seem that left hand terms in Eq. 3 should be disregarded, and the thermal conductivity alone was governing the temperature spatial distribution [12]. With these propositions the Eq.3 can be solved in polar coordinates (r, z):

$$T_e(r,z) = T_{e0}\cdot \exp\left(-0.4\frac{z}{R}\right)\cdot J_0^{2/7}\left(2.4\sqrt{\frac{r}{R}}\right) \qquad (8)$$

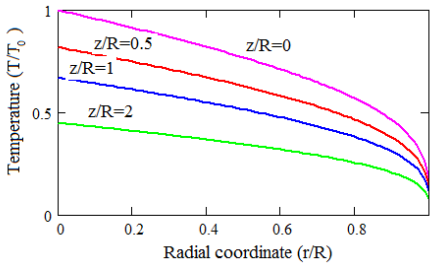

Figure 5. Electron temperature spatial distribution.

Two important remarks should be made regarding this solution (Eq.8). It was obtained with two border conditions: $T=T_0$ at r, z=0 and T=0 at r=R=D/2. However, plume plasma becomes collissionless at $r<<D$, and Eq.(3) cannot be applied in the area $r\sim R$. And, implementing the other type of border conditions by defining temperature and its derivatives at the origin of coordinate system produces additional problems that do not have clear physical solution (for details, see Ref. 11). Thus, electron thermal conductivity causes the decrease in electron temperature with the distance from thruster exit. In order to apply Eq.8 to the far field plasma one should introduce a physical process decreasing electron free path on a few orders of magnitude, and only then the electron

thermal conductivity itself can cause the drop in electron temperature below 1 eV observed in a far field [9,15-17]. The basic idea was expressed in Ref. 18, and its development is shown below.

Total current emitted by floating plasma thruster is equal to zero, and it means that in vacuum chamber electron and ion currents toward the walls are equal:

$$\oint j_{ew}(r)dS = \oint j_{iw}(r)dS \qquad (9)$$

The simplest solution of Eq (9) (but not unique) is the equality of local current densities:

$$j_{ew} = j_{iw} \qquad (10)$$

For a flat wall, electron current density is

$$j_{ew} = en_{ew}\cdot\left(\frac{T_e}{2\pi m_e}\right)^{1/2} \qquad (11)$$

And ion current density is

$$j_{iw} = en_{iw}\left(\frac{2e\Phi_b}{m_i}\right)^{1/2} \qquad (12)$$

Equations for ion and electron "liquids" and electrostatic potential in 1-D model can be written as following[19]:

$$\frac{d}{dy}n_{e,i}v_{e,i} = 0 \qquad (13)$$

$$\frac{d}{dy}\left(m_{e,i}n_{e,i}v_{e,i}^2\right) = -\frac{d}{dy}n_{e,i}T_e \pm en_{e,i}\frac{d\Phi}{dy} \qquad (14)$$

$$\frac{d^2\Phi}{dy^2} = 4\pi e\left(n_e - n_i\right) \qquad (15)$$

Average ion charge is set to Z=1 for simplicity, and $T_e >> T_i$.

Eqs.13-15 are valid for $0 \le y < y_b$, and y_b is the distance from wall where quasi neutrality is restored.

Disregarding for bulk motion of electrons and suggesting isothermal electrons one can obtain quite simple equations for densities and plasma potential:

$$n_e(x) = n_{ew}\exp(\Psi) \qquad (16)$$

$$n_i(x) = n_{iw}(1-\beta\Psi)^{-1/2} \qquad (17)$$

$$\frac{d^2\Psi}{dx^2} = \exp(\Psi) - \frac{\alpha}{(1-\beta\Psi)^{1/2}} \qquad (18)$$

In Eqs.16-18 the following dimensionless variables and parameters are introduced:

$$\Psi = \frac{\Phi}{T_e} \ge 0; \quad x = y\cdot\left(\frac{4\pi n_{ew}e^2}{kT_e}\right)^{1/2}; \quad \alpha = \frac{n_{iw}}{n_{ew}}; \quad \beta = \frac{2T_e}{m_i v_{iw}^2}$$

Border conditions are obvious: at x =0 Ψ=0.

The first integral of Eq.18 is

$$\frac{1}{2}\left(\frac{d\Psi}{dx}\right)^2 = \frac{1}{2}E_w^2 - \frac{2\alpha}{\beta} - 1 + \frac{2\alpha}{\beta}\cdot(1-\beta\Psi)^{1/2} + \exp(\Psi) \qquad (19)$$

Here E_w is dimensionless electric field strength normal to the wall.

Parameter α can be found from Eqs. 10-12 (Xenon ions):

$$\alpha = \left(\frac{m_i}{4\pi m_e\Psi_b}\right)^{1/2}$$

The results of numerical integration of Eq.19 are shown in Fig.6.

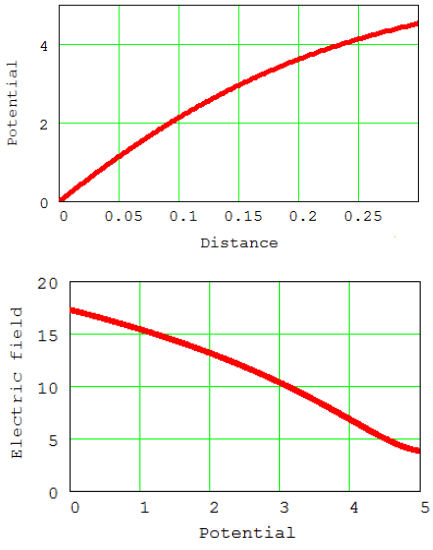

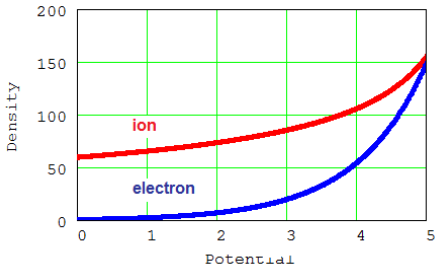

Figure 6. Potential distribution, electric field, and ion and electron densities are shown for a model with α=60, β=0.17, $E^2{}_w$=600.

Dimensional distance from the wall to the bulk plasma is:

$$y_b = 0.3\cdot\alpha^{1/2}\left(\frac{kT_e}{4\pi m_e e^2}\right)^{1/2} \approx 2\,mm$$

$$for\ n_e = 10^7 \quad cm^{-3}, T_e = 1 \quad eV$$

Thus, very thin layer of separated charges can provide necessary balance of ion and electron currents.

Ion life time in chamber can be estimated as

$$\tau_i = \left(\frac{m_i}{2e\Phi_b}\right)^{1/2} L \approx \left(\frac{m_i}{10T_e}\right)^{1/2}\cdot L$$

In order to support current balance the life time of an electron should be the same. The length of electron trajectory in chamber can be estimated as

$$l_e = \left(\frac{2T_e}{m_e}\right)^{1/2}\cdot\tau_i = \left(\frac{m_i}{5m_e}\right)^{1/2}\cdot L \approx 220L \qquad (20)$$

It is seen in Fig.4 that the length of trajectory (Eq.20) is equal (or even larger) than free path for electrons at temperatures around 1 eV and densities of $10^7 - 10^8$ cm^{-3}. In such case, the Eq.4 and solution (8) are applicable and can be confronted with experimental data. For example, the experiment with floating SPT-100 thruster [2] demonstrated the decrease of electron temperature from 2.6 eV to 1 eV along the radial distance of 70 cm. These numbers could be considered as qualitative agreement with theoretical results in Fig.5. According to calculations (Fig.6) bulk plasma potential should be equal to $5T_e$ approximately. Again, experimental data [2] confirmed this relation. Measurements of SPT-50 plasma parameters in relatively small chamber [9] resulted in electron temperatures of 0.5-0.7 eV and plasma potentials of 3-6 V, which agreed with theoretical estimates within factor less than two. Tests of 20 kW ion thruster in significantly larger chamber revealed plasma potentials about 2 V and electron temperatures of 0.25-0.35 eV in the region of far field plasma close to the chamber wall (y=0.2-2.5 m) [15-17].

Of course, one cannot expect a quantitative agreement between simple 1-D model and experimental data obtained for different thrusters in vacuum chambers of widely varied dimensions, but these calculations support conclusion regarding unavoidable influence of chamber walls on spatial distributions of plasma parameters even for experiments with very low neutral gas pressures.

4. ELEMENTARY PROCESSES

An essential difference between orbital reality and ground simulation is the spatial distribution of neutral atoms. When thruster works in orbit, the neutral gas density decreases with distance from exit according to the formula:

$$N_{Xe}(r) = N_0\Omega\frac{D_0^2}{4r^2} \qquad (21)$$

For example, solid angle for SPT-50 was equal to Ω=0.4.

Number of collisions for an electron with neutrals can be estimated as

$$\tau_{eXe}(\varepsilon) = \int_{D_0/2}^{\infty}\sigma_{eXe}(\varepsilon)N_{Xe}(r)dr \approx \sigma_{eXe}(\varepsilon)N_0\Omega\frac{D_0}{2} \qquad (22)$$

In case of ground experiment, the neutral gas pressure in a far field is determined by the balance of flow rate in thruster and pumping speed. Usually, pressure gage is installed on a chamber wall, and Xenon number density can be calculated from available data:

$$N_{Xe} = \frac{p_{Xe}}{kT_{Xe}} = 3\cdot10^{10}p_{Xe}\left(\frac{T_{Xe}}{300K}\right)^{-1} cm^{-3} \qquad (23)$$

Here the pressure is expressed in units of μTorr. Thus, number of collisions in ground chamber should be increased (compared to Eq.22) on

$$\Delta\tau_{eXe}(\varepsilon) = \sigma_{eXe}(\varepsilon)\frac{p_{Xe}}{kT_{Xe}}R \qquad (24)$$

The ratio of these numbers is

$$\delta(p_{Xe}, R) = \frac{\Delta\tau_{eXe}(\varepsilon)}{\tau_{eXe}(\varepsilon)} = \frac{2p_{Xe}R}{kT_{Xe}\Omega D_0} \qquad (25)$$

It follows from Eq.25 that relative number of collisions increases with increasing ratio of chamber dimension to the thruster orifice diameter.

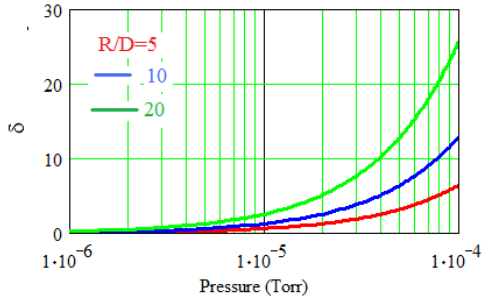

Figure 7. Ratio of number of collisions vs. pressure for R/D_0=5, 10, and 20. $N_0=3*10^{12}$ cm^{-3}, T_{Xe}=500 K.

It is seen in Fig.7 that vacuum chambers with neutral gas pressure over 20 μTorr do not provide a quite adequate environment for testing the interaction of plume plasma with a solar array coupon. In order to calculate the number of collisions with neutral atoms one needs to know the dependence of cross section on energy (see Eqs.22 & 24). According to [20] the cross section has a minimum at ε=0.7 eV ($\sigma(0.7)=2\cdot10^{-16}\,cm^2$), and it grows rapidly to $\sigma(6)=5\cdot10^{-15}\,cm^2$. In the chamber with dimensions of 2 m and pressure of 100 μTorr the numbers of collisions are $\Delta\tau_{eXe}(4eV)=10$, and $\Delta\tau_{eXe}(2eV)=2$. Thus, if vacuum pump provides pressure below 10 μTorr electrons with energies of interest do not experience elastic collisions with xenon atoms. Due to very high ratio of masses $\frac{M_{Xe}}{m_e}=2.4\cdot10^5$ elastic collisions of electrons with neutral atoms cannot change their energy or, in other words, to cause cooling of electron component even with accounting for much higher length of trajectory (Eq.20). Excitation and ionization cross-sections are below $5*10^{-16}$ cm^2 for electron energy in the range of 9-100 eV [21, 22], which means that energy losses for electrons caused by inelastic collision with xenon atoms are negligibly low. Really, the rate of ionization/excitation for *e+Xe* collisions can be calculated from well known cross-sections [21, 23]:

$$\langle\sigma v_e\rangle=\frac{\int_{8.3}^{\infty}\sigma(\varepsilon)\cdot\left(\frac{2}{m_e}\right)^{1/2}\varepsilon\cdot\exp\left(-\frac{\varepsilon}{T_e}\right)d\varepsilon}{\int_0^{\infty}\varepsilon^{1/2}\cdot\exp\left(-\frac{\varepsilon}{T_e}\right)d\varepsilon} \qquad (26)$$

The results are shown in Fig.8.

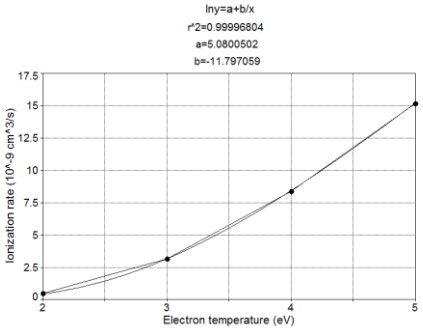

Figure 8. The rate of ionization/excitation for e+Xe collisions.

The atomic number density is equal to $N_{Xe}=2*10^{11}$ cm^{-3} at the pressure of 10 μTorr and temperature of 500 K. Thus, the energy losses for electrons caused by collisions with neutral atoms can be characterized the following mean free paths:

$$l_{eXe}=10^6\,cm^{-3}\quad at\,T_e=2eV,\qquad l_{eXe}=5\cdot10^4\,cm^{-3}\quad at\,T_e=5eV.$$

It is obvious from estimates above that even for the worst chamber conditions (~100 μTorr) the mean free path exceeded chamber dimensions on three orders of magnitude (for 2 eV electrons).

In principle, the difference between thruster plume plasma parameters in space and vacuum chamber could be caused by charge-exchange (CEX) processes. In space, CEX processes are localized inside thruster channel and in near field plasma. The presence of background gas in a vacuum chamber results in the possibility of CEX processes on a wider spatial scale, and this may change the spatial distribution of plasma parameters. According to Ref.24 the respective cross sections can be presented in the following form:

$$\sigma_{CEX}=A-B\cdot\log\varepsilon \qquad (27)$$

This dependence is depicted in Fig.9 for singly and doubly charged ions.

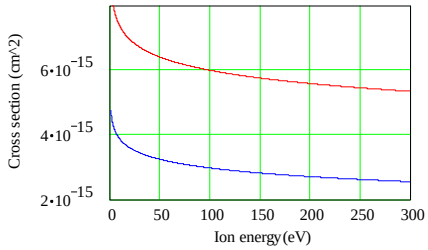

Figure 9. CEX processes cross sections are shown for singly (top) and doubly (bottom) ionized xenon atoms.

Within the range of ion energies of 150-300 eV CEX cross section is approximately $\sigma_{CEX}=5\cdot10^{-15}\,cm^2$

Mean free path for a fast ion is

$$l_{CEX} = \frac{1}{\sigma_{CEX} N_{Xe}} = 0.9 \cdot 10^4 \cdot p_{Xe}^{-1} \quad cm \qquad (28)$$

Thus, in case of high background pressure (20- 100 μTorr) the mean free path is comparable with chamber dimension, and this can be the reason behind high electron number density in area near the walls. Experiment in large chamber demonstrated significant increase in CEX ion densities caused by higher background pressure: ion current density almost doubled when pressure increased from 4 μTorr to 13 μTorr [2]. However, high ion number densities cannot explain low electron temperatures (below 1 eV) observed in ground experiments [9,17]. Electrons could be cooled down by collisions with water molecules and excitation of molecular rotational levels.

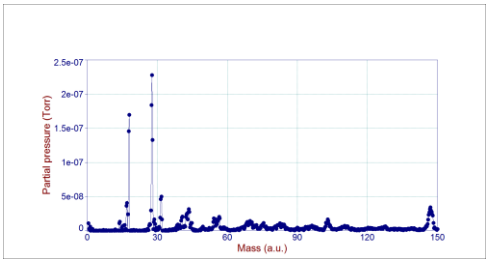

Figure 10. One example of RGA scan in experiment [9].

There are no data concerning water vapor partial pressures for a majority of experiments under discussion. But, measurements performed in Tenney chamber indicated variations of partial pressures within the range of 0.17-4.4 μTorr for H_2O, and 0.2-0.8 μTorr for N_2 (Fig.10). According to Ref. 25 the total cross section for rotational levels excitation depends on electron energy and reaches $\sigma_{eW} = 10^{-14} cm^2$ for electrons with energy around 1 eV. Mean free path for electrons is

$$l_{eW} = \left(\sigma_{eW} \cdot \frac{p(H_2O)}{kT_W} \right)^{-1} = \frac{3 \cdot 10^3}{p(H_2O)} cm \qquad (29)$$

Pressure in Eq.(29) is expressed in μTorr, and temperature is equal to 300 K.

It is seen in Eq.(29) that mean free path is shorter than the length of trajectory (Eq.20), and excitation of rotational levels of water molecules may cool electrons in plume plasma. This might be the reason behind very low electron temperature in Tank 6 test because the chamber was equipped with diffusion pumps [15-17]. If water vapor partial pressure were about 4 μTorr then mean free path would be comparable even with chamber dimensions.

One more complication is introduced to the study by the presence of magnetic field in the chamber (and in LEO). Real trajectory of electron is spiral with the length of a path

$$R_{eff} = \frac{eBR^2}{(32\pi m_e k T_e)^{1/2}} \qquad (30)$$

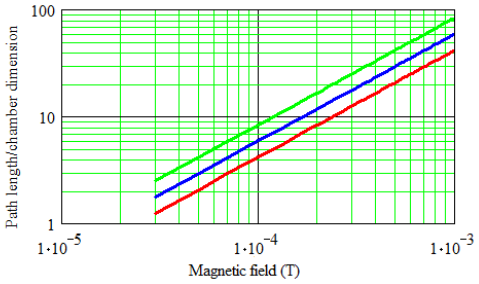

Figure 11. Ratio of real path length to the chamber dimension vs. magnetic field strength (R=2 m, T_e=1, 2, and 4 eV).

It is seen in Fig.11 that the length of the electron trajectory in a chamber with radius *R*=2 m is really three times longer for 1 eV electrons even under Earth magnetic field of 0.3 G. There are no data regarding magnetic field map in vacuum chambers at distances $r >> D_0$. Combining results showed in Fig. 4 and Fig. 11 one can conclude that under field of 0.5 G electrons with energy of 2 eV turn into collisionless at the density of $5*10^9$ cm^{-3}. Thus, magnetic field in the chamber may cause additional cooling of electrons compared to the situation in GEO.

5. CONCLUSIONS.

Plume plasma electron temperature is very important parameter for evaluating the interactions between spacecraft elements and thruster plume. All measurements performed in vacuum chambers indicated rather low electron temperatures (0.5-2 eV) in far field while computer simulations and measurements in space (one only) pointed to significantly higher temperatures (2-6 eV). There are a few mechanisms for cooling electrons in plasma chambers, and they should be taking into account while designing ground tests revealing interactions between plume plasma and spacecraft elements.

6. REFERENCES

1. Brophy, J.R., Gershman, R., Strange, N., Landau, D., Merrill, R.G., and Kerslake, T. “300-kW Solar Electric Propulsion System Configuration for Human Exploration of Near-Earth Asteroids”, AIAA Paper 2011-5514, July 2011.
2. Diamant, K.D., Liang, R., and Corey, R.L. “The

Effect of Background Pressure on SPT-100 Hall Thruster Performance", AIAA Paper 2014-3710, July 2014.

3.Walker, M.L.R., Victor, A.L., Hofer, R.R., and Gallimore, A.D. "Effect of Backpressure on Ion Current Density Measurements in Hall Thruster Plumes", *Journal of Propulsion and Power*, Vol. 21, No.3, 2005, pp.408-415.

4. Foster, J.E., Kamhawi, H., Haag, T., Carpenter, C., and Williams, G.W. "High Power ECR Ion Thruster Discharge Characterization", NASA/TM-2006-214035, February 2006.

5. Beal, B.E., Gallimore, A.D., Haas, J.M., and Hargus Jr., W.A. "Plasma Properties in the Plume of a Hall Thruster Cluster", *Journal of Propulsion and Power*, Vol.20, No.6, 2004, pp.985-991.

6. Dannenmayer, K., Mazouffre, S., Merino, M., and Ahedo, E. "Hall Effect Thruster Plume Characterization with Probe Measurements and Self-Similar Fluid Models", AIAA Paper 2012-4117, July 2012.

7. Herman, D.A., Shastry, R., Huang, W., Soulas, G.C., and Kamhawi, H. "Plasma Potential and Langmuir Probe Measurements in the Near-field Plume of the NASA-300M Hall Thruster", AIAA Paper 2012- 4115, July 2012.

8. Guerrini, G., Michaut, C., Dudeck, M., Vesselovzorov, A.N., and Bacal, M. "Characterization of Plasma Inside the SPT-50 Channel by Electrostatic Probes", IEPC 97-053, October 1997.

9. Vayner, B.V. " SPT-50 Test in VF 20", Internal Report, August 2012 (unpublished).

10. Cohen-Zur, A., Fruchtman, A., and Gany, A. "The Effect of Pressure on the Plume Divergence in the Hall Thruster", *IEEE Transactions on Plasma Science*, Vol.36, No.5, 2008, pp.2069-2081.

11. Huismann, T.D., and Boyd, I.D. "Advanced Hybrid Modeling of Hall Thruster Plumes", AIAA Paper 2010-6525, July 2010.

12. Ashkenazy, J., and Fruchtman, A. "Plasma Plume Far Field Analysis", IEPC-01-260, October 2001.

13. Mikellides, I.G., Jongeward, G.A., Katz, I., and Manzella, D.H. "Plume Modeling of Stationary Plasma Thrusters and Interactions with the Express-A Spacecraft", *Journal of Spacecraft and Rockets*, Vol.39, No.6, 2002, pp.894-903.

14. Baranov, V.B., and Krasnobaev, K.B. "*Hydrodynamic Theory of Space Plasma"*, Moscow, Nauka, 977, p.40.

15. Galofaro, J., and Vayner, B. "High Power Electric Propulsion Characteristics: Vacuum Facility Ground Testing", AIAA Paper 2007-3877, June 2007.

16.Vayner, B., and Galofaro, J. "Plume Plasma Parameters of 20 kW Plasma Thruster", AIAA Paper 2007-4387, June 2007.

17. Vayner, B. "Far Field Plasma Parameters of 20 kW Plasma Thruster", 7th Workshop on Frontiers in Low Temperature Plasma Diagnostics, Bishop Burton College, Beverley, UK, April 1-5, 2007.

18. Katz, I. *Private communications*, 2015.

19. Goebel, D.M., and Katz, I. "*Fundamentals of Electric Propulsion: Ion and Hall Thrusters*", John Willey & Sons, Inc., Hoboken, New Jersey, 2008, pp.78-88.

20. Yuan, J., and Zhang, Z. "Low-energy electron scattering from Kr and Xe atoms", *Journal of Physics B*, Vol.22, 1989, pp.2581-2588.

21. Hayashi, M. "Determination of electron-xenon total excitation cross-sections", *Journal of Physics D: Applied Physics*, Vol.18, 1983, pp.581-589.

22. Syage, J.A. "Electron Impact Cross Sections for Multiple Ionization of Kr and Xe", Physical Review A, Vol.46, 1992, pp.5666-5680.

23. NIST atomic data, Appendix D: "Ionization and Excitation Cross Sections for Xenon".

24. Miller, J.S., Pullins, S.H., Levandier D.J., Chiu, Yu., and Dressler, R.A. "Xenon charge exchange cross sections for electrostatic thruster models", *Journal of Applied Physics*, Vol.91, No.3, 2002, pp.984-991.

25. Faure, A., Gorfinkiel, J.D., and Tennyson, J. "Electron-impact rotational excitation of water", *Monthly Notices of Royal Astronomical Society*, Vol. 347, 2004, pp.323-333.